BULLETIN OF THE EARTHQUAKE
RESEARCH INSTITUTE
Vol. 48 (1970), pp. 29-51

3. *Faulting Associated with the Matsushiro Swarm Earthquakes**.

By Yukimasa TSUNEISHI and Kazuaki NAKAMURA,

Earthquake Research Institute.

(Read Oct. 22, 1968. — Received Nov. 29, 1969.)

Abstract

Ground cracks associated with underground faulting first appeared in the Matsushiro area on April 11, 1966, during the highest seismic period of the Matsushiro swarm earthquakes. Field and instrumental surveys revealed that the fault can be traced for more than 5 km and that its maximum amount of displacement is about 50 cm of left-lateral slip. The surface trace of the fault comprises a number of fissure zones which are made up of numerous en-échelon ground cracks; the fissure zones themselves are arranged in an en-échelon pattern within the larger fissured area. The displacement paths and the rates of displacement were obtained by instrumental measurements. Displacements on fissure zones proceeded in direct correlation with seismic activity and other crustal deformations. In this paper, results of instrumental measurements are summarized, and the relationships of the fault movements to the earthquakes are discussed from a geological viewpoint. Further, the role of groundwater which might have affected tectonic processes, including the seismicity and crustal deformation, is examined.

1. Introduction

The Matsushiro swarm earthquakes, which commenced August 3rd, 1965, still continue, although the frequency has much lowered after a prolonged activity of four years. Various aspects of the earthquakes have been studied by many investigators of different organizations (Morimoto, 1967; Hagiwara, 1967; Hagiwara and Iwata, 1968; JMA, 1968). We have been engaged in the study of surface faulting associated with the earthquakes, and the initial results were successively published as the first and second papers in this bulletin (Nakamura and Tsuneishi, 1966, 1967).

In the first paper, we described the ground cracks in the epicentral area as of June, 1966. The results of field observations and the preliminary instrumental measurements of the cracks could not be in-

*) Ground cracks at Matsushiro probably of underlying strike-slip fault origin, III.

terpreted as indicating a surficial origin, but instead suggested a left-lateral strike-slip movement on a fault below the surface layer to the northeast of Mt. Minakami. In the second paper, the results of observations in the field and by the revised instruments, up to October of 1966, were described. The previously inferred undergound faulting had become all the more plausible on the basis of these results, as well as because of various additional studies including the electro-optical measurement of distance, triangulation, and focal mechanism studies. The trend and the amount of displacement of the "Matsushiro earthquake fault" were estimated.

In this 3rd paper, we present a later result of displacement measurements up to March of 1967. We also summarize features of the fault, especially the mode of development of ground cracks, the amount of displacement, and the dimensions of the fault. We then compare these features with other observational facts of the earthquakes and associated events, including crustal deformation. The movement along the fault still continues at a much reduced rate of several millimeters per year (Tsuneishi, 1968).

Geologic setting

The geology of Matsushiro and the surrounding area is briefly summarized below, based on various earlier studies (Iijima, N., 1962; Morimoto et al., 1966; Kimura, 1967; Matsuda et al., 1967; Sawamura et. al., 1967; Kobayashi, 1968; Iijima and Saito, 1968; Nakamura, 1969a).

The Matsushiro seismic area is located in the northern part of the Fossa Magna, where volcanic and clastic sediments accumulated to a thickness of several thousand meters during the Neogene period. To the west of the northern Fossa Magna stretches the Hida mountains, which reach 3,000 m in altitude. This region is underlain by pre-Cenozoic rocks, mainly Paleozoic clastic rocks and Mesozoic granite. The boundary between the Fossa Magna and the Hida mountains is a great fault zone, the Itoigawa-Shizuoka tectonic line (Fig. 1).

Subsidence of the northern Fossa Magna began in early Miocene, accompanied by submarine volcanic activity. In middle to late Miocene, intrusion of diorite-porphyrite occurred in a belt crossing the sedimentary basin in a NE-SW direction. Since then, the belt has become comparatively rigid and has become an uplifted block (the central belt of uplift; Iijima, N., 1962). The belt was later partly covered by subaerial volcanics of Pliocene and Pleistocene age.

In the sedimentary basin to the southeast of the central belt of uplift, non-marine Pliocene sediments accumulated, whereas in the basin to the northwest of the belt the accumulation of thick marine sediments continued through Miocene to Pliocene time. The strata in the north-

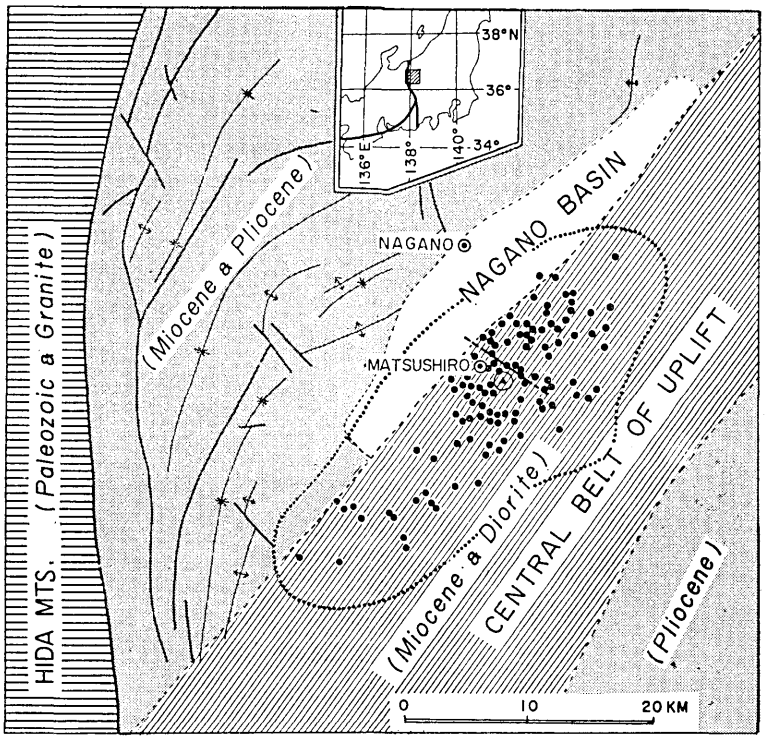

Fig. 1. Simplified tectonic map, inluding the epicentral distribution of the major shocks and the realm of ultra-micro earthquakes. For details see text.

western basin were later folded and faulted. The structural trend seems to have been controlled by both the Itoigawa-Shizuoka tectonic line and the central belt of uplift. The folding movement is considered to be still active, as is indicated by late Quaternary deformed terraces and by the results of precise levelling. Sedimentation still continues in the Nagano basin, which lies between the northwest basin and the central belt of uplift. Electrical sounding reveals that in some places the unconsolidated sediments attain 200 m in thickness (Ono, 1967).

The present relief of the central belt of uplift is mountainous, attaining elevations greater than 2,000 m. On the northwestern rim of the belt, coalescent alluvial fans have developed at the foot of the mountains and in the wider valleys. Their deposits attain thicknesses of 100 m at the maximum. The town of Matsushiro lies on such alluvial fans and on the alluvial plain of River Chikuma, which flows along the northwestern border of the central belt of uplift. The belt is characterized by numerous historic swarm earthquakes and scattered hot springs.

Outline of the earthquake sequence

The graph showing the frequency of the Matsushiro earthquakes, as

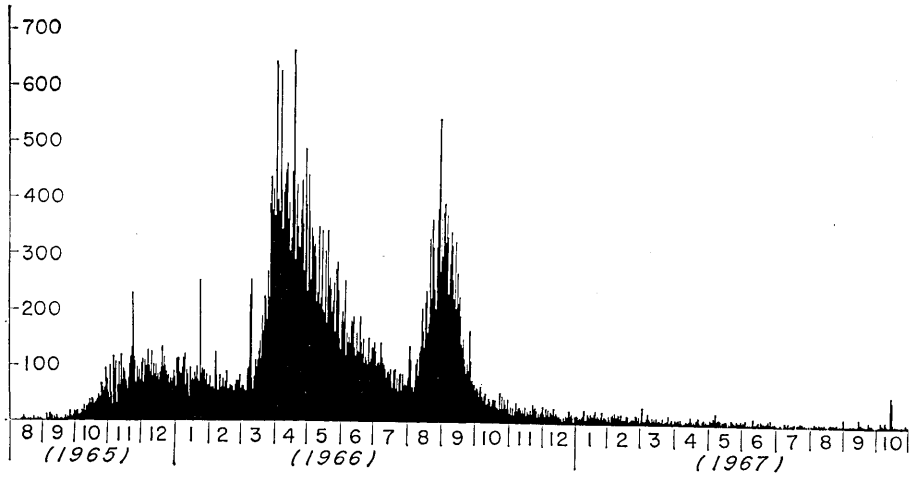

Fig. 2. Daily frequency of felt earthquakes registered at Matsushiro Seismological Observatory, JMA (location in Fig. 4).

recorded at Matsushiro Seismological Observatory of the Japan Meteorological Agency, is reproduced in Fig. 2 (JMA, 1968). The observatory is situated near the center of epicentral area (Fig. 4). Three peaks of seismicity are recognized through the whole period, in November of 1965, in April of 1966, and in August-September of 1966. The third peak was associated with the most conspicuous crustal deformation, and the frequency curve of this peak is symmetrical as compared to the previous ones.

The epicenters of the earthquakes had been restricted in a circular area about 12 km in diameter centered around Mt. Minakami until July of 1966. After this time the seismic area gradually enlarged to the northeast and to the southwest and finally became an ellipse with a long axis of 34 km. The focal depth of most earthquakes ranges between 2 and 7 km below the surface. The maximum magnitude is 5.1, and the total energy released through November of 1967 is 1.66×10^{21} ergs, which corresponds to the energy of a single earthquake with a magnitude of 6.3 (Hagiwara and Iwata, 1968).

The distribution of epicenters of major earthquakes, as shown in Fig. 1, is restricted to the northwestern half of the central belt of uplift, although the epicentral area of minor earthquakes occupies a slightly larger area. The underground structure of the central belt of uplift was revealed by an explosion seismic study (Asano et al., 1969). According to the study, the top of the third layer with a velocity of 6.0 km/s, is very shallow and extends to a depth of about 1 km under the belt. On the other hand, the depth of the interface becomes deeper by a few kilometers under the surrounding basins. Most of the foci of the

present earthquakes exist within the layer with the velocity of 6.0 km/s.

It was in April of 1966—the highest seismicity period—when the surface trace of the fault first appeared distinctly on the surface as ground cracks. In late August mineral water of 10^7 m^3 in approximate volume began to well out extensively within the faulted area and its surroundings (Iijima, H., 1969), and it caused several landslides from the middle of September to early October, when the rate of welling was highest (Morimoto et al., 1967).

2. Development of surface faulting

The Matsushiro earthquake fault is recognized on the ground surface as an assemblage of minute ground cracks arranged in double échelon and by a number of deformed man-made structures. Following is a brief summary of the development of surface faulting, more fully described in previous papers (Nakamura and Tsuneishi, 1966, 1967).

Terminology on ground cracks used in our present and previous papers is illustrated in Fig. 3. The elementary constituent of *ground cracks*, which is used as a general term, is a simple *crack* up to several meters long, which is regarded as being formed essentially by tension fracture. Regular en-échelon arrangement of these cracks constitutes a *fissure zone* of 100-700 meters length. There are right-lateral and left-lateral fissure zones in the sense of horizontal displacement, which is indicated by the mode of en-échelon arrangement. In addition, the left-lateral fissure zones are distributed en échelon in a narrow belt named *fissured area*. We inferred a buried left-lateral strike-slip fault below this belt (Fig. 4). Thus the surface trace of faulting is double échelon in pattern, inasmuch as the zones of en-échelon cracks are themselves distributed in an en-échelon pattern within the fissured area.

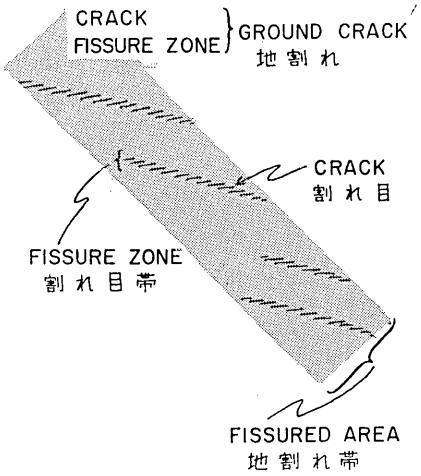

Fig. 3. Terminology used in this paper for ground cracks.

Four left-lateral fissure zones, F1-F4, appeared during the April peak of seismicity, whereas the other twelve zones were formed during the August-September peak. Three right-lateral zones are distributed along the northeastern margin of the fissured area (Fig. 4).

After the middle of August, 1966, vertical displacements along the fissure zones became distinct. The northern side along the left-lateral

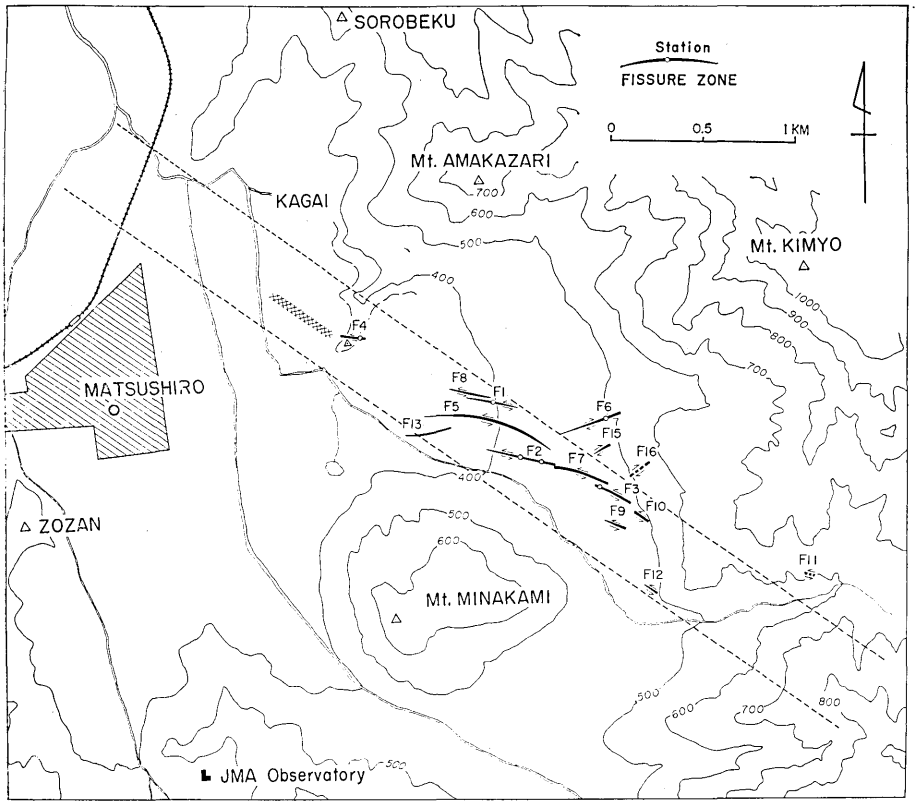

Fig. 4. Fissure zones formed by underground faulting, and stations for displacement measurements.

fissure zones and the southern side along the right-lateral ones subsided by a maximum amount of 30 cm. A bore hole drilled 3 m north of the left-lateral fissure zone F1 penetrated the fissure zone between 34.8 m and 41.9 m depth. Therefore, the fissure zone dips 86° to the north, with about 60 cm width, assuming that the hole is vertical.

The formation of ground cracks is greatly controlled by the surficial geology. All of the above-mentioned ground cracks developed on the surface soil of alluvial fans with the exception of one small bedrock hill. The northwestward extension of the fissured area is characterized by a low, wet, and flat alluvial plain developed along the River Chikuma, and is not apparently preferable for the formation of ground cracks. Instead, the buried fault is recognized here by the systematic deformation of long man-made structures, such as concrete dikes of rice-fields, road-side ditches, underground water pipes, and railway tracks. Their breakages are distributed linearly in a NW direction on the extension of the fissured area. The characteristic mode of breakage is that the structures which are oriented in an approximate N-S direction

are selectively pulled apart.

In the epicentral area, a number of ground cracks of landside and simple vibrational origin were formed in addition to the cracks of fault origin (Morimoto et al., 1967; Tomizawa, 1969).

3. Displacement along fissure zones

As described in the previous chapter, the surface expression of the Matsushiro earthquake fault is not that of a single shear plane, but is an assemblage of numerous ground cracks which are distributed in a belt of about 500 m width. We traced the displacement along the fissure zones by daily measurements at six stations, successively set up as the new zones appeared (Fig. 4). The displacement along the buried fault as a whole can be estimated by the results thus obtained and by geodetic and other means.

At most of the stations we measured the two horizontal components but not the vertical component of displacement. This is mainly because the latter component was negligible during the earlier stage. The vertical component, however, became appreciable after the middle of August, 1966, and it resulted in a tilting of the measurement plane of horizontal components to various degrees. But the effect of tilting on our measurement was small, so that we can discuss the mode of horizontal displacement on the basis of our measurements.

The methods used were described in detail in our previous papers. Only a brief summary is given here. If a fissure zone crosses a man-made structure, such as a concrete slab, the displacement of the zone is concentrated in a few cracks within the structure. In this case we measured the displacement of cracks with the aid of a slide caliper. On the natural ground surface without man-made structure, we set up steel rods, steel pipes, invar wires or steel tapes which connected piers installed on opposite sides of the fissure zone. Measurements were made with a slide caliper on the pier, and the results were then corrected for temperature.

Six stations on five of the fissure zones are shown in Fig. 4. Daily observation were made in co-operation with residents of Matsushiro. The description of each station with the method adopted and the result of measurement are summarized below, with some necessary repetitions of data from previous papers. Displacement paths shown in Figs. 6, 8, 9 and 10 are represented as the relative motion of the southern side to the northern side across the fissure zone.

Takehara Station on F1

The Takehara station is located on the middle point of fissure zone F1.

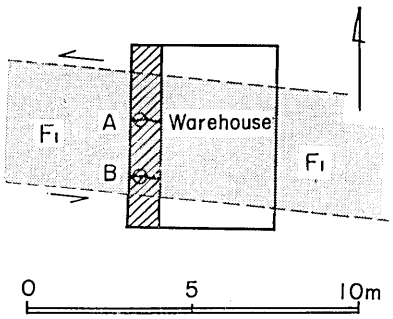

Fig. 5. Sketch map of Takehara station on F1. **A** and **B** show the locations of displacement measurements on the broken concrete slab in front of the warehouse.

The zone, or at least a part of it, was formed on April 11, and the measurements started on April 22. At the station the zone, with the width of 3 m, crossed a 520 × 90 cm concrete slab in front of a warehouse and broke the slab into three segments. The slab covers the total width of the fissure zone (Fig. 5).

Four reference points, which were positioned at each corner of a square with sides of about 15 cm long, were set across northern crack A and southern crack B on the slab, respectively, as illustrated in the lower insert in Fig. 6. The lengths of the sides and diagonals of the squares across the cracks were measured to the nearest 1/20 mm.

Movements of two points, I and II, relative to the northern base line were calculated by trigonometry (Fig. 6). The difference of displacements of points I and II indicates rotation of segments of the slab.

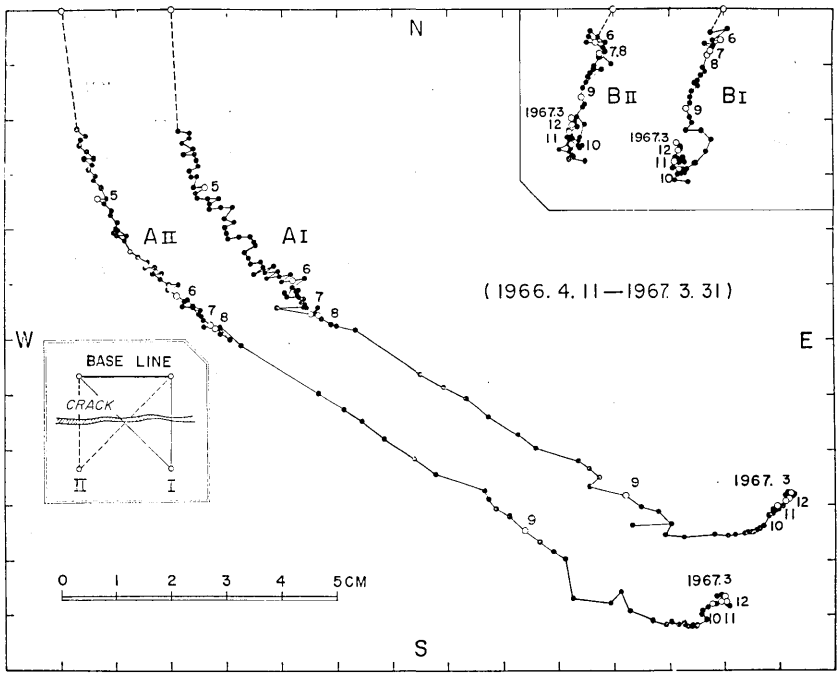

Fig. 6. Displacement paths of cracks **A** and **B** on the concrete slab at Takehara station on F1. For details see text

In fact the slab, which was divided into three segments, has deformed into an S-shape by the left-lateral movements across the fissure zone. In Fig. 7 the upper figure, A_I-A_{II}, represents a counter-clockwise rota-

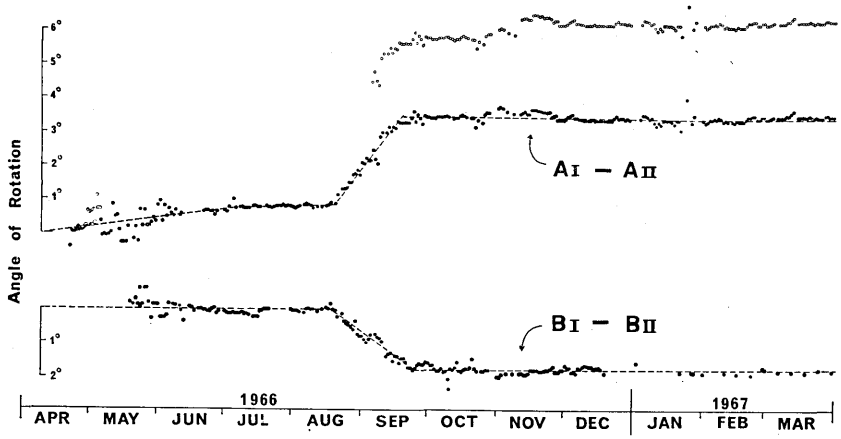

Fig. 7. Angle of rotation of the fractured concrete slab at Takehara station on F1.

tion of the middle segment relative to the northern one, whereas B_I-B_{II} represents clockwise rotation of the southern segment relative to the middle one. Open circles in A_I-A_{II} of Fig. 7 represent actual observational values, but they were shifted downward to the position of the closed circles, so as to keep continuity of the curve. The discontinuity is considered to have been caused by a non-tectonic phenomenon, such as accidental pushing-out of the neighboring distorted warehouse, because the discontinuity did not appear in other observational data at this and other stations.

The total displacement of the fissure zone F1 was calculated by combining displacements of the two cracks and rotations of segments of the slab. The obtained displacement path is shown in Fig. 8. The result obtained by rough direct measurement of the fractured slab (in

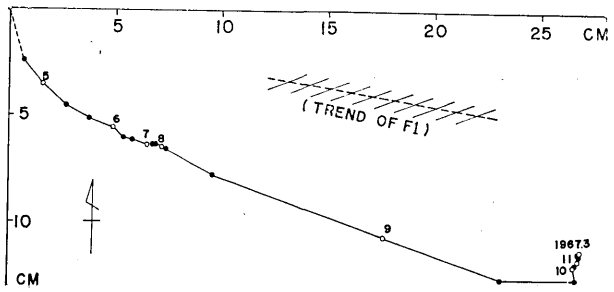

Fig. 8. Reconstructed displacement path of the left-lateral fissure zone F1 at Takehara station.

our second paper, p. 439) gave similar values indicated in the figure. The dotted line connected to the origin in Fig. 8 represents the amount of displacement before the beginning of our measurements. The cumulative amount of strike-slip and opening of the fissure zone is shown in Fig. 11.

Seseki Station on F2

Two stations were set up on the fissure zone F2, but only the result on the western station is presented in this paper. The zone, which first appeared on April 17, crossed a wooden house and broke its concrete foundation in two places. Because of the arrangement of the two cracks, we can estimate the total displacement of the zone by summing the displacements on each crack. Separation of cracks was measured to the nearest 1/20 mm between reference points installed on opposite sides of the cracks.

The results shown in Fig. 11 represent the sum of displacements of the two cracks. The trend of the fissure zone is N 80° W and that of the ruptured edge of the concrete foundation is N 30° W.

Ikedanomiya Station on F4

The fissure zone F4 traverses a hill which is composed of Miocene rocks, whereas all other zones appeared on alluvial fans. The station is located in the yard of a shrine on the east flank of the hill. The measurements were made by the extensometer of stainless steel pipe which was described as Type III-v in our second previous paper.

Two parallel rows of ground cracks were formed about 4 meters apart at this station. The equipment was set across the northern row. We estimate that the observed displacements represent about half of the total displacement of the zone.

Our measurements commenced on June 18 (one month after the date of discovery), when the minimum amounts of 3 cm left-lateral slip and 3 cm separation were observed across the surface cracks.

The displacement path and its changes with time are shown in

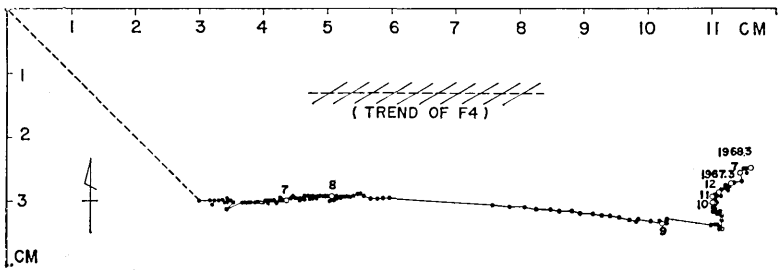

Fig. 9. Displacement path of the left-lateral fissure zone F4 at Ikedanomiya station.

Figs. 9 and 11, respectively. In this station an automatic creepmeter of invar wire type was also installed. The resulting measurements are shown in Fig. 12.

Sugama Station on F6

Fissure zone F6 is a right-lateral zone which is located on the northeastern side of the fissured area. The measurements were carried out by a steel tape and by an extensometer which was of the same type as that used on F4. At this station the fissure zone was composed of four rows of ground cracks in a zone about 10 m wide. The stainless-steel-pipe extensometer was set across the northernmost row of cracks, and the base lines for measurements by steel tape covered the entire width of the zone.

The observed displacement paths are shown in Fig. 10. The steel-

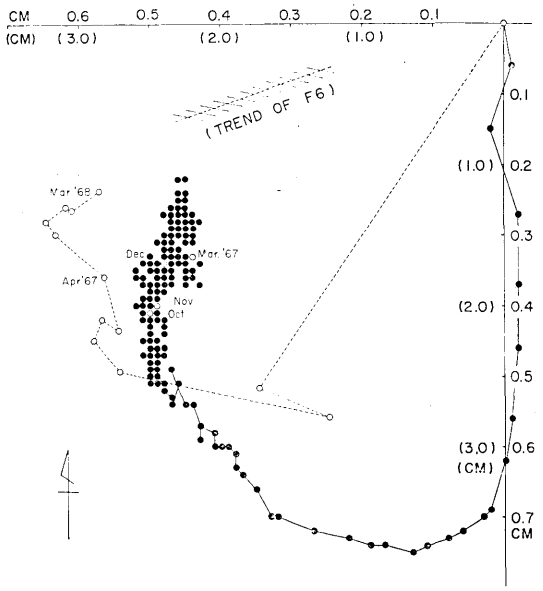

Fig. 10. Displacement path of the right-lateral fissure zone F6 at Sugama station. Solid circles are the results by the stainless-steel-pipe extensometer. The dotted line with open circles represents measurements by steel tape of base lines which extended across the entire width of the fissure zone (scale in parentheses).

tape measurements were about five times larger than those made by the extensometer. Changes in the amount of displacement are shown in Fig. 11.

Summary of displacements across fissure zones

Characteristic features of displacements across fissure zones are

summarized below, based on the results obtained by the measurements described in the preceding sections.

The changes in amounts of displacement with time at different stations are nearly the same in gross pattern as that of the rise and fall of seismicity, as shown in Figs. 11 and 14. This indicates that the movements of individual fissure zones were caused by a common origin, possibly by fault movement.

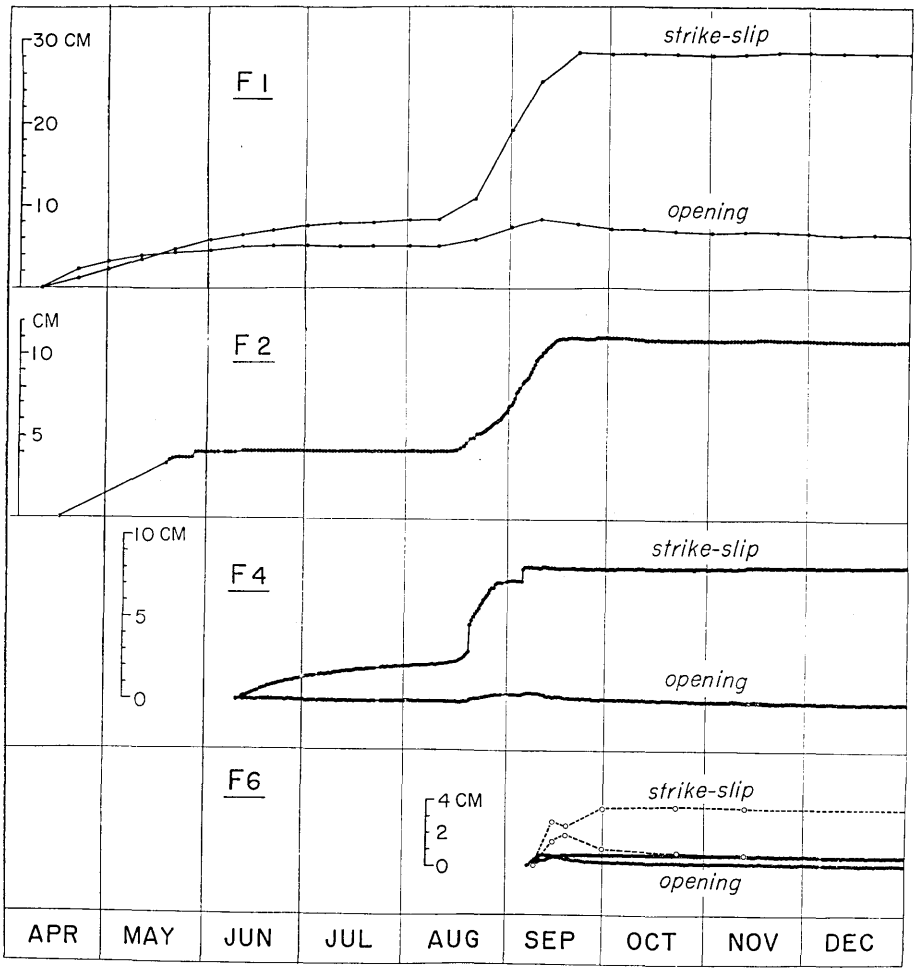

Fig. 11. Cumulative displacements across the fissure zones F1, F2, F4 and F6.

As to the displacement paths in the horizontal plane, three stages are recognized in all the zones that we measured: the first stage when opening movement proceeds together with increasing strike-slip displacement, the second stage of predominant strike-slip movement, and the last stage of minor closing movement. The three stages do not proceed

simultaneously in different zones. For example, in early September F6 was in the first stage while F1 and F4 were in the second stage. Therefore, this type of change of displacement path is associated with the characteristics of individual fissure zones themselves rather than with the mode of displacement of the fault at depth.

Two different time modes of displacement are recognized, as is shown in Fig. 11. One is a gradual increase and the other is an abrupt jump. This difference is significant even when we take into account that the interval of our measurements was once or twice a day and that the precision was one tenth of a millimeter. There are as yet no available data concerning the possibility that the apparent gradual increases might consist of a series of smaller jumps.

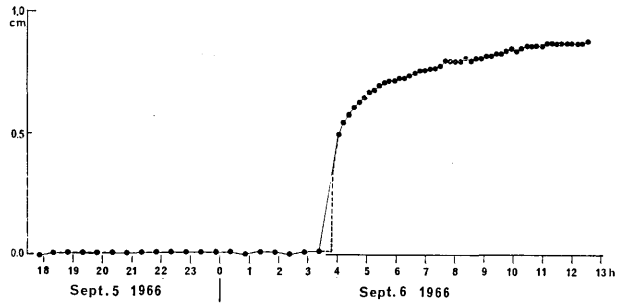

Fig. 12. Displacement associated with an earthquake with a magnitude of 4.9 (No. 60 in Table 1) observed at Ikedanomiya station on F4 (reproduced from Fig. 40, Nakamura and Tsuneishi, 1967).

The most distinct abrupt increases of displacement were observed on August 20 and September 6 at F4. They were apparently caused by earthquakes with the hypocenters nearly on the fault plane. The jump on September 6 was traced in more detail by an automatic creepmeter of invar wire type. Fig. 12 shows that the displacement starts abruptly at the time of the earthquake and then gradually decreases in rate for several hours. This implies that the observed displacement is a direct result of the same underground faulting that caused the earthquake. That is, the fault movement which started at a depth of 5.2 km propagated to the ground surface.

Fig 13 shows, as solid circles, the hypocentral distribution of the three earthquakes which caused jumps in surface displacement (Table 1). Inasmuch as these earthquakes are all included in the major earthquakes listed by Hagiwara and Iwata (1968), the rest of the earthquakes in the list are plotted as open circles; these shocks occurred from April 11, when the first surface faulting appeared, to December, 1966. Solid circles with a white dot in the center show earthquakes which occurred

on April 11 and 17, when openings of ground cracks were noted by residents. Some of these nine earthquakes (e.g. Nos. 19, 20, 21, 26 and 28) are probably responsible for the observed openings, which would correspond to jumps in displacement. We conclude that those earthquakes which caused jumps in surface displacement could be distributed on the fault plane, taking into account the accuracy of hypocentral determination.

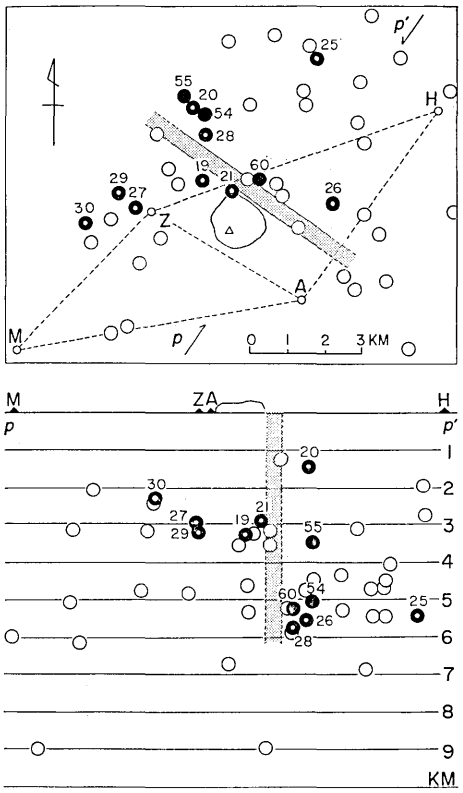

Fig. 13. Distribution of major earthquakes during the period April 11 to December 31, 1966. Earthquakes which are presumed to have been associated with surface faulting are marked as described in the text.

At the Ikedanomiya station on F4, strike-slip movement proceeded even during the period of low seismicity in July of 1966, when the movement at most other stations apparently came to a halt. The same relation has been observed since middle September, 1966. The peculiarity of the displacement at this station is considered to result from the local geological environment at the station. Because the station lies almost directly on Tertiary rocks, it can reflect sensitively the fault movement in the underlying basement rocks. On the other hand, slow response or partial absorption of displacement apparently has occurred at the other stations, which instead lie on thick alluvial fan deposits.

4. Size of the Matsushiro earthquake fault

The fissured area that is defined by the distribution of fissure zones is 500 m wide and 3 km long (Fig. 4). The region southeast of the known fissured area is mountainous, and we could not find any ground cracks, partly because of thick vegetation and rocky, steep slopes. However, a few new mineral springs were discovered on the projected fault trace which were of the same chemical composition as those that appeared in the fissured area. On the other hand, toward the northwest there stretches a flat alluvial plain where, in spite of the absence

Table 1. List of earthquakes which are presumed to have been associated with surface faulting. The original data are from Hagiwara and Iwata (1968).

No.	Date	h m	d (km)	M
19	1966 Apr. 11	04 : 57	3.4	4.5
20	11	04 : 58	1.5	4.5
21	11	06 : 06	3.0	4.5
25	Apr. 17	10 : 21	5.5	5.0
26	17	10 : 22	5.6	4.1
27	17	15 : 46	3.0	4.4
28	17	20 : 02	5.8	4.4
29	17	20 : 06	3.2	4.3
30	17	20 : 28	2.3	4.2
54	Aug. 20	19 : 50	5.1	4.4
55	20	19 : 50	3.5	4.4
60	Sept. 6	03 : 37	5.2	4.9

of soil cracks, we could find several breakages of man-made structures by faulting, as described in chapter 2 and also in our second paper (pp. 448–458). The length of the entire zone is 5 km, including such surface features probably indicative of a buried fault.

Horizontal, left-lateral deformation was recognized still farther northwest by triangulation performed by the Geographical Survey Institute (GSI, 1967). Thus an area of over 7 km length is regarded as directly influenced by faulting.

The strike of the fault is N 55° W, and the dip of the fault plane is presumably nearly vertical, as suggested by the focal distribution of those earthquakes which caused the jumps in displacement described in the previous chapter (Fig. 13). The fault is considered to attain a depth of 5 km, based on the same data. The vertical attitude of the fault plane is also supported by focal mechanism studies.

The maximum amount of horizontal fault displacement is inferred to be roughly 50 cm and 30 cm, in left-lateral strike-slip and opening components, respectively, from the following various data.

Sorobeku and Mt. Minakami (Fig. 4) are the triangulation points which are located outside of and nearest to the fissured area. The relative movements of the two points, which were associated with the present earthquakes, are 98 cm and 80 cm in components parallel and perpendicular to the trend of the fault, respectively. They probably represent the largest possible amount of fault displacement, because the two points are located about 1 km away from the outer margin of the fissured area. Thus the amount should comprise both the elastic

and non-elastic deformation of the material, which exists between the fault and the triangulation points, in addition to the amount of the fault displacement itself.

An estimation of the fault displacement is also obtained by our measurement of fissure zones. If a line perpendicular to the trend of the fault is drawn through the station on F1 (Fig. 4), the line crosses another zone F5 near its middle point. The maximum amount of displacement along the zone F5, which was attained at the middle point, is almost the same with that of the zone F1 (Table 1 in our second paper, 1967). Twice the amount obtained at the station on F1 (left-lateral slip of 56 cm and opening of 16 cm) will thus roughly indicate the amount of fault displacement (Fig. 8.)

To the northwest of fissure zone F4, a concrete roadside ditch of 100 m length was fractured and stretched by 40 cm, as described in our second paper. Inasmuch as the ditch is N 10° W in trend, and makes an angle of 45° with the fault, both left-lateral slip and opening along the fault could stretch the ditch. The extension of the ditch of 40 cm thus corresponds to 57 cm of pure left-lateral slip or 57 cm of pure opening along the fault.

The fault crosses the straight portion of the track of the Nagano Electric Railway, which here trends N 20° E. Left-lateral slip of 20～30 cm and extension of 36 cm in this direction were observed within a 500 m section of the track. The fraction of extension due to left-lateral slip is estimated as 8 cm, and the remaining 28 cm extension corresponds to 29 cm of opening along the fault.

The amount of the vertical displacement attains some 15 cm of subsidence of the northern side, judging from the results of precise-levelling (Tsubokawa et al., 1967). This value is smaller than the maximum vertical displacement (about 30 cm) observed on the fissure zones. This indicates that the ground surface tilted locally near the fissure zones. The following consideration may explain the difference of values. Because the fissure zones possibly dip to the north, as observed in the bore hole drilled on F1, the northern hanging walls of the zones may collapse or bend downward into the open fissures, resulting in an additional apparent vertical displacement close to the fault.

5. Comparison with other observational data

In Fig. 14 seismicity is expressed in ten-day averages of the number of felt earthquakes resistered at Matsushiro Seismological Observatory (JMA in Fig. 4), and the fault displacement is represented by the results observed at the Takehara station on F1. Correlation is obvious

between the periods of high rates of displacement and periods of high seismicity.

Repeated observations of crustal deformation in the epicentral area include precise levelling (Tsubokawa et al., 1968), electro-optical measurement of distance (Kasahara et al., 1968) and tilt measurement (Hagiwara, 1967). Maximum amounts of observed crustal deformation are a N-S extension of 115 cm, an E-W compression of 22 cm, and uplifting of 86 cm.

Change of horizontal displacement is represented by that of the base line crossing the assumed fault between Mt. Minakami and Sorobeku (Fig. 4). In order to represent vertical deformation, the movement of bench mark C, which is located 1 km northeast of the triangulation point Mt. Minakami, is shown relative to bench mark No. 3661 situated near the point M in Fig. 13. Measurements of ground tilting in Fig. 14 are the result of water-tube tiltmeters installed at JMA observatory (Fig. 4). These crustal deformations and fault displacements show quite similar changes. High rates during the August-September seismic peak and slight reversals in the subsequent period are particularly evident.

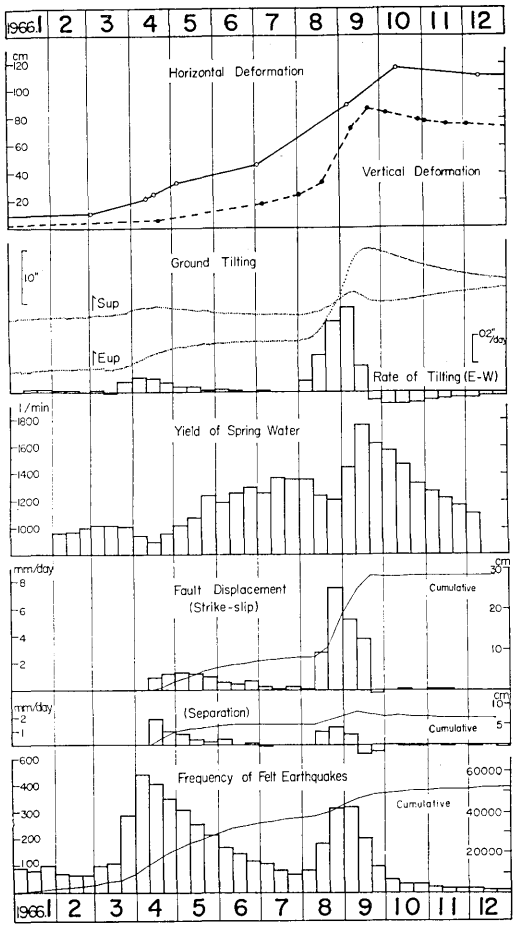

Fig. 14. Comparison of various types of observational data.

A vast amount of ground water, which was rich in calcium, natrium and chlorine and oversaturated with carbon dioxide, welled out throughout the fissured area and its surroundings for a few months after the end of August (Morimoto et al., 1967; Kitano et al., 1967). This phenomenon was also observed at existing springs as an increase in discharge and as a change of chemical composition. Results obtained at one such spring (Kasuga, 1967), located 2 km northwest of Mt. Minakami at

Kagai (Fig. 4) are shown in Fig. 14 as an example. The discharge observed in 1966 has a single peak in mid-September, when the sense of most of crustal deformations began to reverse. There are two minimum in April and August when the seismicity attained its maximum values.

6. Discussion

A prime peculiarity of the Matsushiro earthquake fault is that it is associated with swarm-type earthquakes. Some of the characteristics of the present fault may be attributed to this fact.

There has not been found any pre-existing significant fault in the area of the present faulting from either topographic or geologic studies (Matsuda, 1967). That the surface trace of the fault was double échelon in a zone relatively wide compared to its length can be explained by the newness of the fault. The fissured area might be regarded as an embryonic form of a crushed zone of a fault.

The epicentral distribution of the Matsushiro earthquakes is evidently controlled by the NE-SW geologic structure (Fig. 1), whereas the newly formed fault has a direction of N 55° W, crossing the structural trend at a right angle. Consequently, the number of earthquakes that are directly related to the fault displacement is very limited (Fig. 13).

The characteristic focal mechanism of the present earthquakes is of quadrant type, with maximum compressional axis N 80°~90° E, according to the studies of 87 larger shocks (Ichikawa, 1967) and smaller shocks (PSOMESS, 1966, p. 1711). Consequently, one of the nodal lines corresponds to the strike of the fault. East-west compression is common to earthquakes in the neighboring area (Ichikawa, 1967).

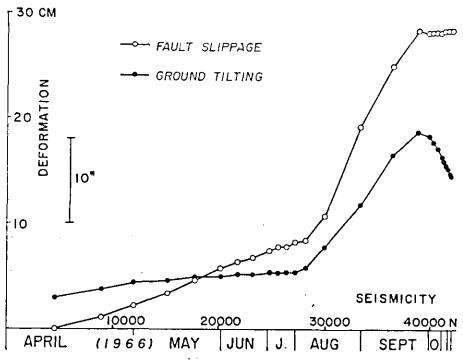

Fig. 15. Relationship between cumulative number of felt shocks and fault displacement and ground tilting.

The August-September peak in seismicity is characterized by a high rate of crustal deformation, as was described in the previous chapter (Fig. 14). Fig. 15 was prepared to show this relation more quantitatively. The axis of seismicity denotes the cumulative number of felt shocks since the beginning of 1966; the fault slippage is the result obtained at station F1; and the ground tilting represents

the results of the E-W component of the water-tube tiltmeter (Fig. 14). The whole period can be divided into three parts which are different in the gradient of the curve, or "efficiency". The second period, August to September, has the highest efficiency. The change of the efficiency from the first period to the second seems to be too sharp to be explained in terms of a gradual change in the mechanical property of the rocks in the focal domain, as might be expected by the accumulated effects of fracturing associated with the earthquakes. The change seems rather to be related to differences in focal depth. The average depth of hypocenters in the second period is shallower by about 1 km than in the foregoing period (PSOMESS, 1966; JMA, 1968).

There seems to be some genetic relation between the abnormal welling out of ground water and the tectonic processes, including the seismicity and crustal deformation. The peak to the abnormal welling in mid-September coincides in time not only with the change of the efficiency in Fig. 15, but also with the change in areal distribution of seismicity. That is, the seismic activity almost ceased after that time in the area along the fault (Hagiwara and Iwata, 1968), and the sense of most of the crustal deformation reversed (Fig. 14).

Two alternative interpretations are possible: (1) the outflow may be interpreted as the result of crustal fracturing, or (2) the water may be a generator of the crustal deformations and earthquakes (Hagiwara, 1967; Nakamura, 1969b), as is supposed in the case of the Denver earthquakes (Evans, 1966).

There are many hot springs in and near the present epicentral area, which is favorable to the first hypothesis in that the existing mineral water under compression in the subsurface flowed out through the newly formed fault plane. On the other hand, the shallower focal domain before the peak in the welling can be regarded as indicating an upward migration of the pressure source of the crustal deformation, which would favor the second hypothesis. The deep drilling now in progress at Matsushiro might be expected to give an answer to the role of ground water in the earthquakes.

Acknowledgement

The authors express their sincere gratitude to residents of Matsushiro, especially Mrs. Makie Saito, Mr. Koichi Aizawa, Mr. Shuichi Ogawara, Mr. Kengo Nakamura and Miss Yasuyo Nishimura for their co-operation in daily measurements, and Mr. Zenji Kumai, Mr. Tomokazu Nakamura and Mr. Yoshiteru Aoki for kindly offering their ground for measurement stations. They are also very grateful to Prof. R.

Morimoto for constant encouragement and facilities, and to Prof. Clarence R. Allen for a critical reading of the manuscript and many valuable suggestions by which the manuscript was much refined. They are also indebted to Prof. T. Kimura for a critical reading of the manuscript.

References

ASANO, S., S. KUBOTA, H. OKADA, M. NOGUCHI, H. SUZUKI, K. ICHIKAWA and H. WATANABE, 1969, Explosion seismic studies of the underground structure in the Matsushiro earthquake swarm area, *Jour. Phys. Earth*, **17**, 77-90.

EVANS, D. M., 1966, Man-made earthquakes in Denver, *Geotimes*, **10** (9), 11-18.

G S I, 1967, Geodetic surveys in the area of Matsushiro earthquake swarm, *Bull. GSI*, **12** (2), 20-25.

HAGIWARA, T., 1967, Geophysical studies of the Matsushiro earthquakes, *Zisin*, **20** (4), 192-200 (in Japanese).

HAGIWARA, T. and T. IWATA, 1968, Summary of the seismographic observation of Matsushiro swarm earthquakes, *Bull. Earthq. Res. Inst.*, **46**, 485-515.

ICHIKAWA, M., 1967, Statistical study of the focal mechanism of Matsushiro earthquake swarm, *Zisin*, **20**, 116-127 (in Japanese with English abstract).

IIJIMA, H., 1969, Surface geology of Matsushiro area and disasters by the Matsushiro earthquake swarm, *Report Coop. Res. Disas. Prev.*, **18**, 103-115 (in Japanese with English abstract).

IIJIMA, N., 1962, Volcanostratigraphy and petrology of the north-eastern part of Fossa Magna (1) — Volcanostratigraphical study, *Bull. Fac. Education, Shinshu Univ.*, **12**, 1-48 (in Japanese).

IIJIMA, N. and Y. SAITO, 1968, Geology of Sarashina-Hanishina area, *Regional Geology of Sarashina-Hanishina area*, **1**, 43-158 (in Japanese).

J M A, 1968, Report on the Matsushiro earthquake swarm, August 1965-December 1967, *Tech. Report JMA*, **62**, 556p. (in Japanese with English abstract).

KASAHARA, K., A. OKADA, M. SHIBANO, K. SASAKI, S. MATSUMOTO and M. HIRAI, 1968, Electro-optical measurement of horizontal strains accumulating in the swarm earthquake area (4), *Bull. Earthq. Res. Inst.*, **46**, 651-661.

KASUGA, I., 1967, Aspect on the relation of thermal water and Matsushiro earthquakes in Kagai hotspring area, Nagano Prefecture, *Jour. Tokyo Geogr. Soc.*, **76**, 76-86 (in Japanese with English abstract).

KIMURA, T., 1967, Structural division of Japan and the Honshu arc, *Jap. Jour. Geol. Geogr.*, **38**, 117-131.

KITANO, Y., R. YOSHIOKA, S. OKUDA and K. OKUNISHI, 1967, Geochemical study of ground waters in the Matsushiro area, Part 1: Chemical composition of ground waters, *Bull. Disas. Prev. Res. Inst. Kyoto Univ.*, **17** (2), 47-71.

KOBAYASHI, K., 1968, Quaternary crustal movements in the inland part of the Fossa Magna, *Mem. Geol. Soc. Japan*, **2**, 33-38 (in Japanese with English abstract).

MATSUDA, T., 1967, Geological aspect of the Matsushiro earthquake fault, *Bull. Earthq. Res. Inst.*, **45**, 537-550 (in Japanese with English abstract).

MATSUDA, T., K. NAKAMURA and A. SUGIMURA, 1967, Late Cenozoic orogeny in Japan, *Tectonoph.*, **4**, 349-366.

MORIMOTO, R., 1967, Geologic background of the Matsushiro earthquake swarm, *Zisin*, **20** (4), 187-192 (in Japanese).

MORIMOTO, R., I. MURAI, T. MATSUDA, K. NAKAMURA, Y. TSUNEISHI and S. YOSHIDA, 1966, Geologic consideration on the Matsushiro earthquake swarm since 1965 in central Japan, *Bull. Earthq. Res. Inst.*, **44**, 423-445 (in Japanese with English abstract).

MORIMOTO, R., K. NAKAMURA, Y. TSUNEISHI, J. OSSAKA and N. TSUNODA, 1967, Landslides in the epicentral area of the Matsushiro earthquake swarm — Their relation to the earthquake fault, *Bull. Earthq. Res. Inst.*, **45**, 241-263.

NAKAMURA, K., 1969a, Geological provinces in north central Japan in relation to Matsushiro earthquakes, *Trans. Am. Geoph. Union*, **50**, 388-389.

NAKAMURA, K., 1969b, Surface faulting during the Matsushiro earthquakes, *Trans. Am. Geoph. Union*, **50**, 389-390.

NAKAMURA, K. and Y. TSUNEISHI, 1966, Ground cracks at Matsushiro probably of underlying strike-slip fault origin, I — Preliminary report, *Bull. Earthq. Res. Inst.*, **44**, 1371-1384.

NAKAMURA, K. and Y. TSUNEISHI, 1967, Ground cracks at Matsushiro probably of underlying strike-slip fault origin, II — The Matsushiro earthquake fault, *Bull. Earthq. Res. Inst.*, **45**, 417-471.

ONO, Y., 1967, Electrical sounding at Matsushiro earthquake district (I), *Notes Coop. Res. Disas. Prev.*, **5**, 23-27 (in Japanese with English abstract).

PSOMESS, 1966, Matsushiro earthquakes observed with a temporary seismographic network. Part 2, *Bull. Earthq. Res. Inst.*, **44**, 1689-1714.

SAWAMURA, K., T. KAKIMI, M. SOGABE, I. KOBAYASHI and H. HASE, 1967, Geology and geological structure of the Matsushiro seismic area, *Notes Coop. Res. Disas. Prev.*, **5**, 3-11 (in Japanese with English abstract).

TOMIZAWA, T., 1969, On the fissure group caused by Matsushiro earthquake, *Earth Sci. (Chikyu Kagaku)*, **23**, 100-106 (in Japanese with English abstract).

TSUBOKAWA, I., A. OKADA, H. TAJIMA, I. MURATA, K. NAGASAWA, S. IZUTUYA and Y. ITO, 1967, Levelling resurvey associated with the area of Matsushiro earthquake swarms (1), *Bull. Earthq. Res. Inst.*, **45**, 265-288 (in Japanese with English abstract).

TSUBOKAWA, I., A. OKADA, S. IZUTUYA, Y. ITO and K. KADONO, 1968, Levelling resurvey associated with the area of Matsushiro earthquake swarm (2), *Bull. Earthq. Res. Inst.*, **46**, 417-429 (in Japanese with English abstract).

TSUNEISHI, Y., 1968, Recent displacement of the Matsushiro earthquake fault, *Mem. 5th Symp. Disas. Sci.*, 173-175 (in Japanese).

---

3. 松代群発地震にともなつた断層運動

地震研究所 { 恒石幸正 / 中村一明 }

松代群発地震にともなつた断層運動の野外調査および計器観測に従事してきた筆者らは，すでに二度にわたりその結果を報告してきた (Nakamura and Tsuneishi, 1966, 1967). 本稿ではすでに発表された資料に，その後1967年3月までに得られたものを加えて再整理を行つた結果を提出し，他の多くの研究者による成果と合せることにより松代地震断層の地質学的意味，地震活動・地殻変動との関係について若干の考察を加える.

第2図にみられるように松代地震は1965年8月にはじまり，その後同年11月，翌年4月および8—9月と三つの活動期をむかえた. 断層運動による地割れは1966年4月の第2のピークの最中に皆神山北東方に現れた. 地震は第1図にみられるように北部フォッサマグナを横断する中央隆起帯の北西部にそつて分布しており，断層はこの震央域のほぼ中央部に出現している. 中央隆起帯は中新世後期に玢岩・閃緑岩の貫入をうけて固化し，同時に隆起した地域である (飯島南海夫, 1962). 現在この帯の上には多数の温泉が分布し，また有史以来の群発地震の活動が知られている.

松代地震断層は少くも地表では単一の剪断面ではなく，規則的に雁行配列した地割れの集合あるい

は人工構造物の系統的な変形として表現されている．第3図は地割れに対して本稿で用いられる術語の意味を示したものである．まず「地割れ」という語は総称として用いられる．地割れの最小構成単位は「割れ目」とよぶが，これは伸張破壊によつて形成されたと考えられる長さ数 m 程度以下の破壊面である．割れ目は雁行配列することにより「割れ目帯」を構成する．割れ目帯は割れ目の配列様式により水平運動のセンスが区別される．左ずれ割れ目帯はそれ自身再び雁行配列をすることによつて「地割れ地帯」を形成するが，筆者らはこの地帯の地下に左横ずれ断層を推定しているのである．

第4図は割れ目帯の分布を示したものである．点線で示されているように地割れ地帯は約500mの幅をもつている．割れ目帯のうち F1-F4 は地震活動の第2のピークに，他は第3のピークに現れた．割れ目帯にそつた鉛直変位は，左ずれ割れ目帯では北側が，右ずれ割れ目帯では南側が落下している．地割れ地帯の北西延長部は低湿地であるため地割れの発達はみられないが，その代りに人工構造物が特徴的な変形を示しており，地下の断層運動を認めることができる．一方南東方では植生のためや急斜面であること，あるいは土壌が欠けていることにより地割れは観察されないが，地割れを通して湧出したと考えられる新しい温泉の湧き口が存在している．

割れ目帯の変位の観測は第4図に示されている6地点で行われ，変位の方向と変位の時間変化が求められた．人工構造物が割れ目帯を覆つている場所では構造物中に生じたクラックの変位がノギスによつて直接測定された．一方自然の地面の上に割れ目帯が現れている場所ではステンレスパイプ，インバール線，スチールテープなどを媒介として測られた．以下に示す各測点で得られた変位の方向は割れ目帯の北側に対する南側の相対変位として表されている．

第5図は F1 の竹原観測点の見取り図であるが，コンクリート床に二ヶ所のクラックが生じている．第6図の左下に挿入されている図のように各クラックの両側にそれぞれ二個の固定点を設け，クラックを横ぎる測線の長さの変化る測ることにより点 I と II の変位が求められた．その結果は第6図に示されている．同一クラックにおける I と II との変位の差はクラックにより分割されたコンクリート床の回転量を表している（第7図）．クラックの変位と回転量を合成することによつて F1 全体の変位が求められるわけであるが，その結果は第8図に示されている．第9図は F4 上の池田宮観測点での結果，第10図は右ずれ割れ目帯 F6 上の菅間観測点で得られた結果である．F2 上に設けられた二つの観測点のうち西側の瀬関観測点では N 30° W 方向の一測線の観測しか行われなかつたので変位の方向は求められない．以上得られた各割れ目帯の変位の方向をみると開口→横ずれ→閉塞という順序が共通してみられる．しかしこの各段階はすべての割れ目帯について同時に起つているのではない．したがつてこの変位方向の変化は地下の断層運動の変化を直接に反映しているのではなく，地割れに固有な発展段階を表しているものと考えられる．

第11図には各観測点で得られた変位の時間的変化が割れ目帯に平行な成分と垂直な成分とに分けて示されている．各割れ目帯の変位は互いに相似た変化をみせ，また地震活動の消長とも時期的に一致して進行している．さらにこまかくみると F4 では8月20日と9月6日に変位の不連続が起つているが，これは断層上に発生した地震によつて生じたものである．9月6日の飛躍的な変位の進行は F4 上に設置された自動記録変位計でもとらえられた（第12図）．

第13図および第1表には変位の飛躍に関与したと考えられる地震が示されている．8月20日と9月6日のものは黒丸で表示した．中空の黒丸は4月11日と17日に起つた主な地震であり，このうちのいくつかの地震（No. 19, 20, 21, 26 および 28）は当日観察された急速な変位の進行に関係していると思われる．

F4 における変位は他の割れ目帯の変位が事実上停止している1966年7月および10月以後においても着実に進行している．これは他の割れ目帯が厚い扇状地堆積物の上に生じているのに対して，F4 は中新世の岩石からなる丘の上に生じているために，地下における変位の進行を敏感にとらえることができたことによると考えられる．

松代地震断層の長さは 3km の地割れ地帯の他に，その両延長部において断層運動を示唆する地変の起つた地域を含めると約5kmとなる．いつぽう国土地理院によつて行われた三角測量の結果は7km以上にわたつて変動が及んでいることを示している．断層の走向は N 55° W，傾斜は第13図の断層運動に関係した地震の震源分布より判断してほぼ90°である．同様にして断層の深さは 5km にまで達していると思われる．種々の観察事実に基いて推定される大よその変位量は左横ずれ 50cm，断層にそう開口量 30cm，北落ちの鉛直変位 15cmとなる．

第14図は地震活動，および水平・鉛直・傾斜として表される地殻変動，湧水量と断層変位との比較を示したものである．この湧水量は，1966年8月末より数ヶ月間地割れ地帯一帯に炭酸ガスと共に噴き出した Ca, Na, Cl に富んだ異常湧水の変化を示すものである．第14図において断層変位の進行（正確には割れ目帯 F1 の変位）と地震活動との間に明らかな相関がみられるとともに，断層変

位と他の地殻変動の変化とはよく傾向が一致している．湧水量は9月中旬に最大となり，その後は急速に減少しているが，この減少の時期に対応して地殻変動の向きが逆転していることが見てとれる．

第15図はまた地震活動と地殻変動との関係を量的に比較したものである．横軸には有感地震回数の積算が，縦軸には割れ目帯 F1 の積算変位と水管傾斜計による土地の傾斜変化がとられている．地震活動の第3のピークでは第2のピークに比して地殻変動はより能率的に進行しており，しかもその変換は8月はじめに急激に行われている．地震活動の持続とともに地下の岩石の破壊が進行していつた結果として地殻変動がだんだんと効果的に起りうるようになつたという説明では，この急激な変化の説明として不十分であると思われる．むしろこれは第3のピークの震源が以前に比して約1km浅くなつたという事実と関係しているのではなかろうか．

松代地震断層の最大の特徴はそれが群発地震にともなつて出現したことである．この事実は松代地震断層がもつ性質のいくつかを規定しているように思われる．この断層は既存の断層が再動したのではなく，新たに形成されたものであつた．断層の長さにくらべて大きな幅をもつていることは断層の新生という事実に関係しているであろう．松代地震の震源は北東方向にのびる地質構造に支配されて分布しているにもかかわらず，断層は地質構造を分断する方向に現われたということは特異である．したがつて全体の地震のうち一部しか断層変位に直接的に関与していない．しかし多くの地震の発震機構は東西に主圧力方向を向けた四象限型であり，その節線のひとつと断層の走向との一致にみられるように地震を起した応力配置と断層を形成したそれとは等しい．またその応力配置は中部日本に共通しており，松代地震が群発型であるという特殊性をもちながらも全体的な応力場に支配されていることがわかる．

8月末より地割れ地帯に多量に噴き出した異常湧水と地震活動および地殻変動との間には成因的な関係があるように見える．9月中旬に湧水量がピークに達するのに先立つて震源が浅くなり，著しい地殻変動が現われた．湧水がピークに達してのち減少しはじめると地殻変動は逆転し，また断層付近の地震活動は著しく減少した．これらの事実から，間隙水圧が岩石の見かけの剪断強度を低下させるということを考慮しながら，地下水圧の深部における増加が地震および地殻変動の重要な原因のひとつとなつたとする見方が一方では成り立ちうる．しかし他方において，松代地域は温泉地帯であるから地下には被圧された地下水がもともと多量に存在しており，これが新たに生じた断層という通路をとおつて地表へ溢れ出してきたという見方も成り立つ．現在進行中の2000m試錐はこの地下水の役割りに対して何らかの解決の鍵を与えるのではないかと期待されている．

謝辞：この研究にあたつて松代町の方々から多大の御協力をいただいた．とくに斎藤まき江氏，西村泰代氏，相沢耕市氏，小河原修一氏，中村健吾氏は一年近くもの間，毎日割れ目帯の変位を測定してくださつた．熊井善治氏，中村智万氏，青木元光氏は観測装置を設置する土地を心よく貸してくださつた．以上の方々に心から感謝いたします．

また研究の過程において，絶えず激励と御援助を与えられた森本良平教授および原稿を読んで有益な御批判をよせられたカリフォルニア工科大学 Clarence R. Allen 教授，木村敏雄教授，に対して筆者らの心からの感謝の意を表します．